Progress In Electromagnetics Research, Vol. 109, 425–440, 2010

A HIGH ACCURACY CONFORMAL METHOD FOR EVALUATING THE DISCONTINUOUS FOURIER TRANSFORM

C. H. Zhu †

Department of Control Science and Engineering
Harbin Institute of Technology
92 West street, Harbin 150001, China

Q. H. Liu

Department of Electrical and Computer Engineering
Duke University, Durham, NC 27708, USA

Y. Shen and L. J. Liu

Department of Control Science and Engineering
Harbin Institute of Technology
92 West street, Harbin 150001, China

Abstract—A highly accurate, fast algorithm is proposed to evaluate the finite Fourier transform of both continuous and discontinues functions. As the discretization is conformal to the function discontinuities, this method is called the conformal Fourier transform (CFT) method. It is applied to computational electromagnetics to calculate the Fourier transform of induced electric current densities in a volume integral equation. The spectral discrimination in the CFT method can be arbitrary and the spectral range can be as large as needed. As no discretization for the Fourier exponential kernel is needed, the CFT method is not restricted by the Nyquist sampling theorem, thus avoiding the aliasing distortions that exist in other traditional methods. The accuracy of the CFT method is greatly improved since the method is based on high order interpolation and the closed-form Fourier transforms for polynomials partly reduce the error due to discretization. Assuming N_s and N are the numbers

Received 20 August 2010, Accepted 26 October 2010, Scheduled 6 November 2010
Corresponding author: Qing Huo Liu (qhliu@ee.duke.edu).
† Also with Department of Electrical and Computer Engineering, Duke University, Durham, NC 27708, USA.

of sampling points in the spatial and spectral domains, respectively, the computational cost of the CFT method is $O((M+1)N\log_2 L)$, where M is the interpolation order and $L = \frac{N_s-1}{M}$. Applications in the spectral analysis of electromagnetic fields are demonstrated.

1. INTRODUCTION

Fourier transform (FT), as the most important basis for frequency domain techniques, is often encountered in scattering [1–3], radar antennas [4–6] and many other fields in electromagnetics [7–9].

Discrete Fourier transform (DFT) is now the dominant tool to obtain the Fourier spectrum in numerical computation. DFT can be implemented by fast Fourier transform (FFT) algorithms with the computational cost of $O(N\log N)$, where N is the number of sampling points. However, the accuracy of the results obtained with the DFT depends on the analyticity of the function under consideration; it can be sometimes very bad if there are discontinuities in the function [10]. The Nyquist sampling theorem [11] is a mandatory requirement for DFT to work well, i.e., the sampling rate must be at least twice the highest frequency of the function in the spatial domain (or temporal domain). However, nearly all data collected in practice are finite in duration, which means that the function is space-limited (or time-limited) and the highest frequency is infinite for such a function. This causes the aliasing distortions [12]. The frequency resolution and range is decided by the sampling points in FFT. The Chirp-z algorithm [13] can make the frequency resolution and range more flexible; however, since it is still based on the trapezoidal quadrature, when it is used to obtain the Fourier transform, it still suffers from aliasing distortions.

There have been many works done to improve the accuracy in estimating the Fourier transform with a finite duration and discontinuous functions; herein we call this the finite discontinuous Fourier transform. Simonen and Olkkonen [14] use Simpson rule to perform the integration; Zeng [15] proposes linear interpolation for $f(x)$; Morelli [16] uses third-order interpolation for $f(x)$, the input function in the spatial domain; Froeyen and Hellemans in [10] and Beaudoin and Beauchemi in [11] use the reestablishing second- and high-order Taylor expansion to approximate $f(x)$, respectively; Fan and Liu [17] introduce a double interpolation procedure for $f(x)$ and the oscillatory kernel $e^{-j2\pi ux}$, which is extended to multi-dimension in [11]; and [1] has derived an algorithm using high-order interpolation for $f(x)$ with Gauss-Chebyshev-Lobatte (GCL) points. Liu et al. [18] have recently proposed a finite-difference time-domain method that can provide calculations for the desired nonuniform frequency points.

From the point of view of numerical computation, DFT is a trapezoidal quadrature scheme. The discretization is implemented in both the input function $f(x)$ and the oscillatory kernel $e^{-j2\pi ux}$. In this scheme, firstly, in order to represent the oscillating kernel with discrete sample points, there should be at least two points per wavelength (or two points per period) of $e^{-j2\pi ux}$. This is an intuitive explanation of the Nyquist sampling theorem. Secondly, the trapezoidal quadrature can be regarded as using a piecewise linear function to approximate the kernel $f(x)e^{-j2\pi ux}$, and as is well known, a higher-order interpolation can obtain better accuracy. Based on these two observations, a method is proposed in this contribution that uses higher-order interpolation for $f(x)$ and no discretization for the oscillating kernel $e^{-j2\pi ux}$ to obtain the Fourier spectrum. The proposed method can obtain much higher accuracy estimation of the Fourier integral with a low sampling rate, thus overcoming the aliasing phenomenon; it can obtain the Fourier spectrum in a frequency range as large as necessary without satisfying the Nyquist sampling theorem. Moreover, The frequency resolution can be arbitrary.

Section 2 introduces the algorithm of the proposed Conformal Fourier transform (CFT). In Section 3, the algorithm is applied to solve a linear time invariant (LTI) system first, and then used to evaluate the Fourier spectrum of the induced electric current density in a layered medium in electromagnetics with exponential accuracy and low computational time. Section 4 gives the conclusions of this contribution.

2. METHOD

Before the discussion, an important result is shown first. The proof of this can be found in Appendix A.

Lemma 1: The finite Fourier transform of a monomial can be explicitly expressed as

$$\int_{-1}^{1} t^m e^{-j2\pi ut} dt = e^w \sum_{s=0}^{m} \frac{(-1)^{m-s} m!}{(m-s)!} \frac{1}{w^{s+1}} - e^{-w} \sum_{s=0}^{m} \frac{m!}{(m-s)!} \frac{1}{w^{s+1}} \quad (1)$$

where $w = 2\pi ju$, and m is a non-negative integer.

In the following, a highly accurate method is developed for the Fourier transform of discontinuous functions, and the fast computation algorithm is also derived.

2.1. CFT for a Continuous Function

Now we consider the Fourier transform of a discontinuous function $f(x)$. Assume that $f(x)$ is continuous within a finite support domain $[p_0, p_1]$, $p_1 > p_0$ and zero elsewhere. Its continuous Fourier transform $F(u)$ is defined as

$$F(u) = \int_{p_0}^{p_1} f(x) e^{-j2\pi ux} dx \tag{2}$$

We divide the interval $[p_0, p_1]$ into $[x_\ell, x_{\ell+1}]$, where $x_\ell = x_1 + (\ell - 1)\Delta$, $\Delta = \frac{p_1 - p_0}{L}$, $x_1 = p_0$, $x_{L+1} = p_1$, $\ell = 1, 2, \ldots, L$. Approximate $f(x)$ in each element by an M-th order Lagrange interpolation polynomial with interpolation points $\{x_{\ell,k}\}_{k=1}^{M+1}$.

$$f(x)_{[x_\ell, x_{\ell+1}]} \approx P_\ell^{(M)}(x) \tag{3}$$

Substituting (3) into the Fourier integration (2), we obtain

$$\int_{p_0}^{p_1} f(x) e^{-j2\pi ux} dx \approx \sum_{\ell=1}^{L} \int_{x_\ell}^{x_{\ell+1}} P_\ell^{(M)}(x) e^{-j2\pi ux} dx \tag{4}$$

By doing the following change of variables in the ℓ-th element

$$x = at + h_\ell \tag{5}$$

where

$$a = \frac{\Delta}{2},\ h_\ell = \frac{x_{\ell+1} + x_\ell}{2} = x_1 + \left(\ell - \frac{1}{2}\right)\Delta, \tag{6}$$

Equation (4) can be rewritten as

$$\int_{p_0}^{p_1} f(x) e^{-j2\pi ux} dx \overset{w:=j2\pi u}{\approx} a \sum_{\ell=1}^{L} e^{-wh_\ell} \int_{-1}^{1} P_\ell^{(M)}(at + h_\ell) e^{-wat} dt \tag{7}$$

Denoting the interpolation points in $[-1, 1]$ as $\{t_k\}_{k=1}^{M+1}$, the interpolation points $\{x_{\ell,k}\}_{k=1}^{M+1}$ in the ℓ-th element can be obtained by (5). Denoting the interpolation basis function at $\{t_k\}_{k=1}^{M+1}$ as $L_k(t) = \sum_{m=0}^{M} D_m^{(k)} t^m$, there is

$$P_\ell^{(M)}(at + h_\ell) = \sum_{k=1}^{M+1} f(x_{\ell,k}) \sum_{m=0}^{M} D_m^{(k)} t^m \tag{8}$$

Substituting (8) into (7) and then applying Lemma 1, we obtain

$$\int_{p_0}^{p_1} f(x)e^{-wx}dx \approx ae^{-wx_1}\sum_{s=0}^{M}\frac{A_s}{(wa)^{s+1}} \tag{9}$$

where

$$A_s = \sum_{\ell=0}^{L}\alpha_{s,\ell}e^{-wl\Delta}, \quad B_{m,\ell} = \sum_{k=1}^{M+1} D_m^{(k)} f(x_{\ell,k}) \tag{10}$$

$$\begin{cases} \alpha_{s,0} = \displaystyle\sum_{m=s}^{M}\frac{m!}{(m-s)!}(-1)^{m-s}B_{m,1}, \\ \alpha_{s,\ell} = \displaystyle\sum_{m=s}^{M}\frac{m!}{(m-s)!}[(-1)^{m-s}B_{m,\ell+1} - B_{m,\ell}], \ \ell \in [1, L-1] \\ \alpha_{s,L} = -\displaystyle\sum_{m=s}^{M}\frac{m!}{(m-s)!}B_{m,L} \end{cases} \tag{11}$$

Theoretically, if (9) is used to evaluate (2), the result should be accurate if $f(x)$ is a polynomial with the order not large than M in its finite support domain. Let us consider a function

$$f(x) = \begin{cases} x^2 + x + 1, \ x \in [-\frac{1}{2}, \ \frac{1}{2}] \\ 0, \qquad \text{otherwise} \end{cases} \tag{12}$$

Fig. 1 shows the relative error of the spectra evaluated with (9). The computation is performed with Matlab R2009b in double-precision. It is shown that the error become very large when u is near zero, as the interpolation order M increases.

This unreasonable phenomenon is due to the round-off error in computation. Detail about the round-off error can be found in [19]. It can be seen that $\alpha_{s,\ell}$ and A_s will increase in the same order as $s!$ when s increases. This will cause large numerical round-off errors in the floating point computation of (9) when $|wa|$ is small and M is large. We will make use of the Taylor expansion of e^x to overcome this difficulty,

$$e^x = 1 + x + \frac{x^2}{2!} + \frac{x^3}{3!} + \ldots + \frac{x^S}{S!} + \ldots \approx \sum_{s=0}^{S}\frac{x^s}{s!} \tag{13}$$

Substituting (6), (8) and (13) into (7) yields

$$\int_{p_0}^{p_1} f(x)e^{-j2\pi ux}dx \approx ae^{-w(x_1-\frac{1}{2}\Delta)}\sum_{s=0}^{S}A_s^0(wa)^s \tag{14}$$

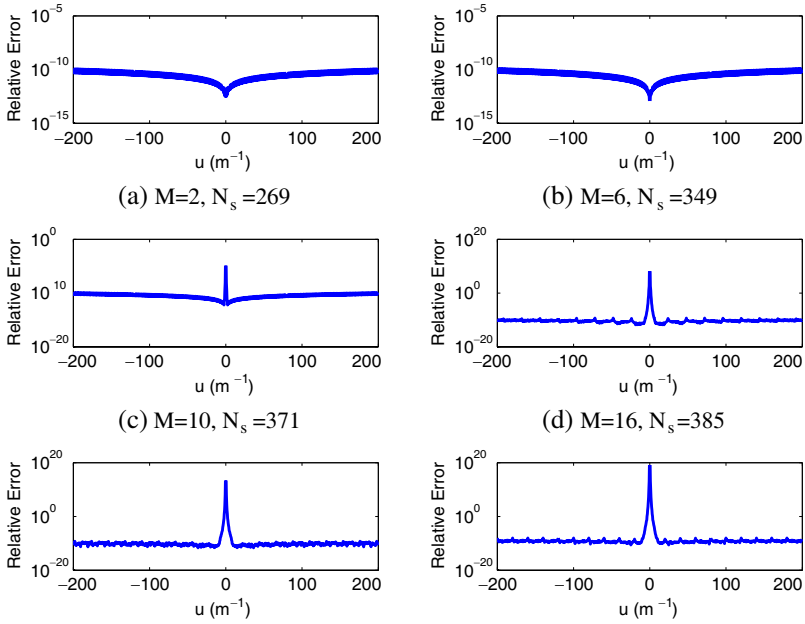

Figure 1. Relative Error of spectra evaluated with (9) for (12). (a) $M = 2$, $N_s = 269$. (b) $M = 6$, $N_s = 349$. (c) $M = 10$, $N_s = 371$. (d) $M = 16$, $N_s = 385$. (e) $M = 18$, $N_s = 397$. (f) $M = 20$, $N_s = 401$.

where

$$A_s^0 = \sum_{l=1}^{L} \alpha_{s,l}^0 e^{-wl\Delta}, \quad \alpha_{s,l}^0 = \sum_{m=0}^{M} \frac{(-1)^s + (-1)^m}{m+s+1} B_{m,l}, \tag{15}$$

In the truncated series in (13), it is reasonable to choose $S = 30$, for $x \leq 3$ in double precision because $\frac{3^{30}}{30!} = 7.7621e-019$. Therefore, with double precision computation, (14) is used if $|wa| \leq 3$; otherwise (9) is used. S can be chosen to be 30. S and the upper boundary of $|wa|$ can be adjusted to obtain proper accuracy. For convenience, we define

$$\mathrm{CFT}_{\mathrm{f,\ L,\ p_0,\ p_1}}(\mathrm{u}) = \begin{cases} ae^{-wx_1} \sum_{s=0}^{M} \frac{A_s}{(wa)^{s+1}}, & |wa| > 3 \\ ae^{-w(x_1 - \frac{1}{2}\Delta)} \sum_{s=0}^{S} A_s^0 (wa)^s, & |wa| \leq 3 \end{cases} \tag{16}$$

We call the method using (16) to compute the Fourier Transform (2)

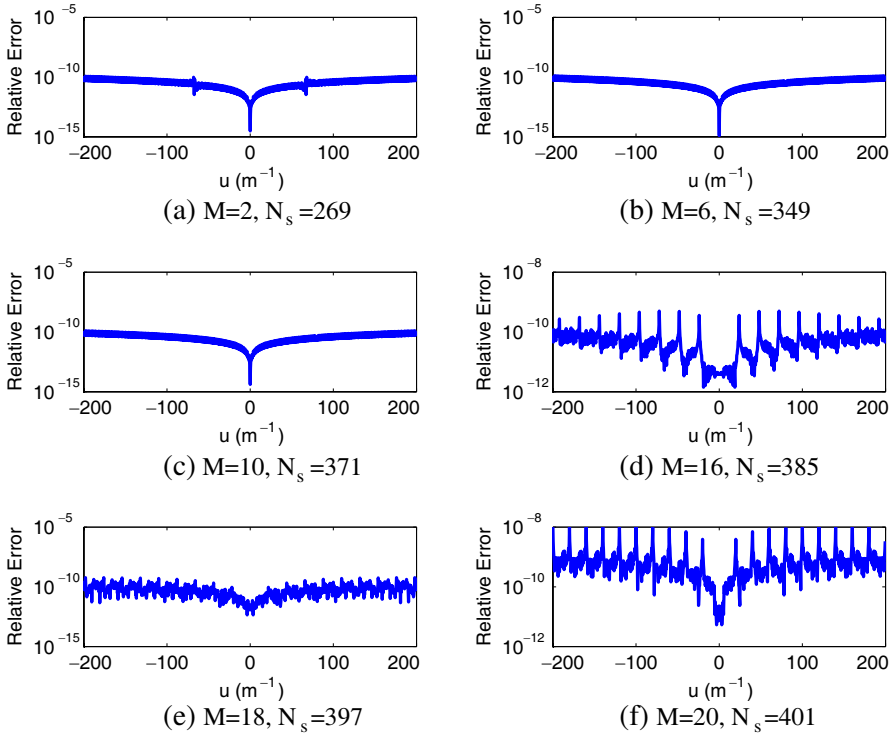

Figure 2. Relative Error of spectra evaluated with (16) for (12). (a) $M = 2$, $N_s = 269$. (b) $M = 6$, $N_s = 349$. (c) $M = 10$, $N_s = 371$. (d) $M = 16$, $N_s = 385$. (e) $M = 18$, $N_s = 397$. (f) $M = 20$, $N_s = 401$.

as the Conformal Fourier transform (CFT). The relative error of the spectrum evaluated with (16) is shown in Fig. 2.

Now, let us discuss the computational cost of the CFT method (16). Suppose the sampling frequency are located at $u = n\Delta f$, $n = -N/2, -N/2+1, \ldots, N/2-1$, where Δf represents the frequency resolution that can be chosen as any number according to the requirement, then N can be chosen according to the interested frequency range. Suppose the the number of u points satisfying $|wa| < 3$ is n_1, then the number of u points satisfying $|wa| \geq 3$ is $n_2 = N - n_1$.

It can be seen that the total number of sampling points in the space domain is $N_s = ML + 1$ when (16) is used, if the interpolation points satisfy $t_1 = -1$, $t_{M+1} = 1$. It requires $O(M^2)$ real multiplications to obtain $\frac{m!}{(m-s)!}$ in (11) and $O[(M+1)^2]$ real

multiplications to obtain $D_m^{(k)}$ in (8) (See Appendix B for the algorithm to compute $D_m^{(k)}$). So the cost of computing $\{\alpha_{s,l}\}_{s=0,l=1}^{M,L+1}$ in (11) is $O(MN_s)$. Equations (10) and (15) are both in the form of chirp z-transform and thus can be computed at the cost of $O((M+1)N\log L)$ and $O((S+1)n_1\log L)$ complex multiplications, respectively [20]. By using the Compensated Horner scheme [21], the results of (9) for u satisfying $|2\pi ua| \geq 3$ can be obtained with $O((M+1)N)$ complex multiplications, and (14) for satisfying $|2\pi ua| < 3$ can be obtained with $O((S+1)n_1)$ complex multiplications. So the computational cost of (16) for CFT is $O((M+1)N\log L)$ complex multiplications.

2.2. CFT for Piecewise Continuous Functions

If $f(x)$ is a piecewise continuous function with the first kind of discontinuity located at $[p_0, p_1, \ldots, p_I]$, making use of (16) in each section, we can obtain the result of CFT for $f(x)$ as

$$F(u) = \sum_{i=0}^{i=I-1} \int_{p_i}^{p_{i+1}} f(x)e^{-j2\pi ux}dx \approx \sum_{i=0}^{i=I-1} \mathrm{CFT}_{f,\ L_i,\ p_i,\ p_{i+1}}(u) \quad (17)$$

It is easy to know that Equation (17) requires $O((M+1)N\sum_{i=0}^{I-1}\log L_i)$ complex multiplications, where L_i is the number of elements in $[p_i, p_{i+1}]$, based on the discussion in part A.

It needs to be pointed out that the only approximation used in deriving (16) and (17) is the Lagrange interpolation for $f(x)$. Since there is no any approximation for the oscillatory kernel $e^{-j2\pi ux}$ term in Fourier transform (2), the algorithm is not restricted by the Nyquist sampling theorem, and therefore, overcomes the aliasing distortion.

3. NUMERICAL RESULTS

Example 1 illustrates how CFT overcomes aliasing distortions under a low sampling density. Then CFT is used to evaluate the Fourier spectrum of an induced electric current density in a layered medium; we show that CFT is fast and can obtain results with high accuracy, and the error has exponential convergence.

Example 1: Consider a stable LTI system characterized by

$$\frac{d^2y(t)}{dt^2} + 4\frac{dy(t)}{dt} + 3y(t) = \frac{dx(t)}{dt} + 2x(t). \quad (18)$$

The output of the system can be achieved by the Fourier method according to the convolution theorem. Assume the input is

$$x(t) = \begin{cases} e^{-t}, & t \in [0, +\infty] \\ 0, & \text{otherwise} \end{cases} \tag{19}$$

First from (18), we know the frequency response of the system is $H(w) = \frac{w+2}{w^2+4w+3}$. The expression of the Fourier transform of input signal (19) can be obtained as $X(w) = \frac{1}{w+1}$. So the Fourier transform of output $y(t)$ is $Y(w) = H(w)X(w) = \frac{w+2}{(w^2+4w+3)(w+1)}$.

$F[y(t)](w)$ is used to represent the Fourier transform of function $y(t)$. So $Y(w) = F[y(t)](w)$. The property of Fourier transform $F[Y(w)](t) = F[F[y(t)]](t) = y(-t)$ leads to $y(t) = F[Y(w)](-t)$. That means $y(t)$ can be obtained through Fourier transform of $Y(w)$.

The results using CFT and FFT both with 321 sampling points in the spatial domain are shown in Fig. 3. The aliasing distortion with FFT can be observed clearly in the figure, as the sampling density used here is lower than the Nyquist sampling density. However, with CFT, we can obtain accurate estimation of the output signal. By increasing the sampling points, we find that 4096 points are needed to obtain 0.48% relative RMS error with FFT; however, CFT requires only 573 sampling points to achieve 0.54% relative RMS error.

Example 2: In electromagnetic analysis, the spectra of sources and fields are often required. Here we consider a plane wave normally impinging on a seven-layer medium with frequency $f_0 = 2\,\text{GHz}$

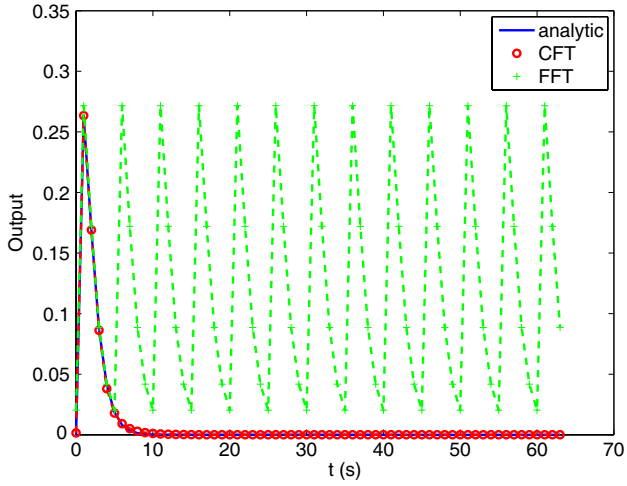

Figure 3. Comparison of the CFT and FFT results for example 1.

in the vacuum background. The layer interfaces are located at [0.1, 0.2, 0.5, 0.7, 0.8, 0.9]; the relative magnetic permeability is 1 for all layers, and the relative permittivity is $\epsilon_1 = 1$, $\epsilon_2 = 32$, $\epsilon_3 = 12$, $\epsilon_4 = 20$, $\epsilon_5 = 40$, $\epsilon_6 = 35$, $\epsilon_7 = 1$, respectively.

The induced electric current density $J(x)$ and its spectral distribution obtained by CFT are plotted in Fig. 4 and Fig. 5. The

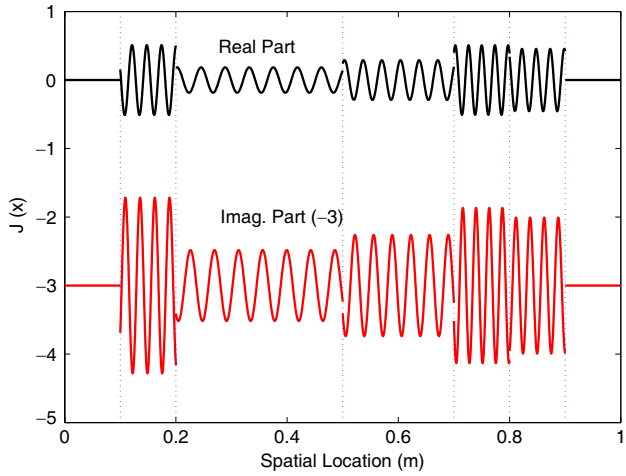

Figure 4. Spatial distribution of an induced electric current density in a seven-layer medium impinged by a plane wave at 2 GHz.

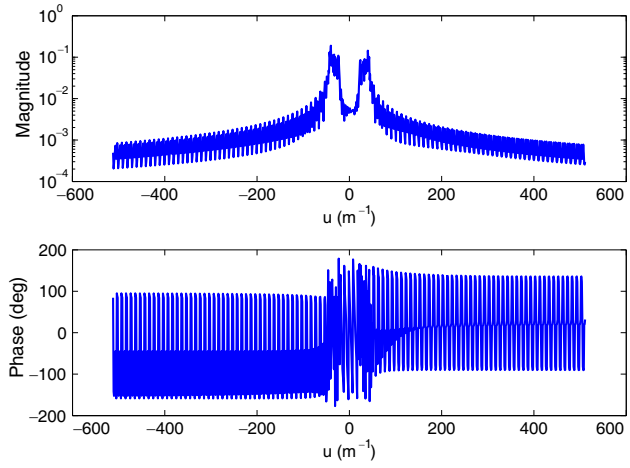

Figure 5. Spectral distribution of the induced electric current density in Fig. 4.

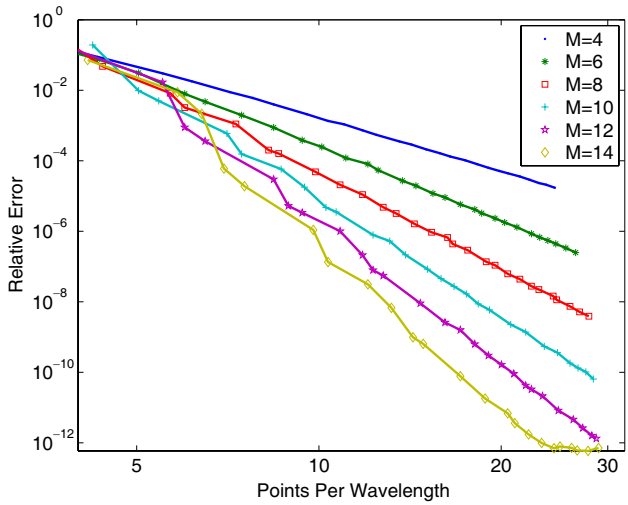

Figure 6. Relative RMS error of the evaluated spectrum by CFT when M is fixed for the problem in Fig. 4.

wave number (spatial frequency) interested are assumed to locate at $u = -512, \ldots, 511$. We use M to represent the interpolating order. Fig. 6, plotted in a log log scale, shows the relative RMS error versus the sampling density in terms of the number of points per wavelength (PPW) when increasing the sampling density with a fixed M. It requires only 5.44 PPW to achieve 0.49% error, 7.45 PPW to achieve 0.016% error, and 10.27 PPW to achieve 0.00047% error using interpolation order $M = 10$.

The above is a typical small problem, and the exponential convergency of CFT error is shown in Fig. 6.

In real applications, often the electrical size is large, namely the domain is much larger than the typical wavelength. Under such circumstances, it can be quite challenging for a traditional method to obtain accurate results. Let us consider a larger scale problem with the same plane wave normal incidence into a large five-layer medium in Example 3. We will compare the performance of CFT with FFT in terms of accuracy, number of sampling points required and the computation time.

Example 3: Consider a plane wave impinges on a five-layer medium with $f_0 = 2\,\text{GHz}$ in the vacuum background. The layer interfaces are located at $[1,\ 4,\ 7,\ 9]$, $\epsilon_1 = 1$, $\epsilon_2 = 3$, $\epsilon_3 = 2$, $\epsilon_4 = 5$, and $\epsilon_5 = 1$; and the wave numbers in the three center layers are 34.6409, 28.2842, 29.8142, respectively.

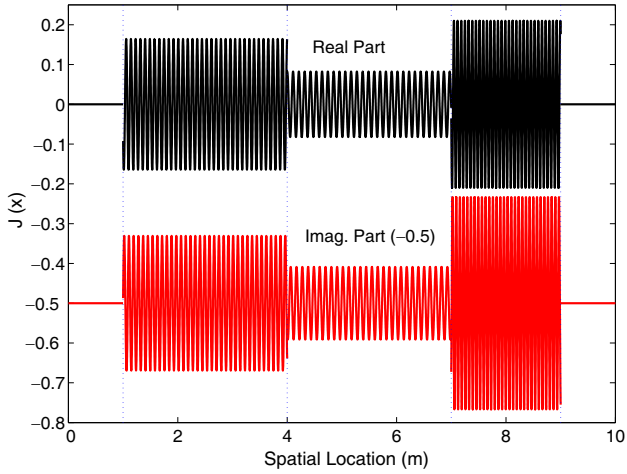

Figure 7. Spatial distribution of the induced electric current density in a large five-layer medium impinged by a plane wave at 2 GHz.

The induced electric current density $J(x)$ is shown in Fig. 7. The frequency interested are assumed to be located at $u = -512, \ldots, 511$. Table 1 shows the comparisons of accuracy, number of sampling points in the spatial domain and CPU time with CFT and FFT. The computation is performed on the same desktop computer with Matlab

Table 1. Error, number of sampling points and run time for CFT and Bluestein's FFT (double-precision).

	Error	N_s	Timing (s)
FFT	1.056×10^{-2}	8192	0.0430
	5.107×10^{-3}	16384	0.0925
	2.534×10^{-3}	32768	0.2007
	6.319×10^{-4}	131072	1.1070
	7.896×10^{-5}	1048576	11.7282
CFT	4.803×10^{-5}	543	0.2768
	2.604×10^{-7}	723	0.3368
	8.601×10^{-10}	1011	0.3569
	9.179×10^{-12}	1605	0.3921

R2009b for double-precision. Bluestein's FFT is used here. With a comparable CPU time, CFT can obtain nearly ten orders of magnitude more accurate than FFT with nearly ten times fewer sampling points. To achieve 7.896×10^{-5} error with FFT, it requires 10486576 sampling points in the spatial domain and the CPU time is 11.7282 s. However, to achieve 4.803×10^{-5} error, CFT requires only 543 sampling points and the CPU time is 0.2768 s; in other words, CFT requires very few sampling points and at the same time, approximately 42 times faster.

4. CONCLUSION

In this contribution, the conformal Fourier transform algorithm as a high accuracy method for evaluating the finite Fourier transform for discontinuous functions is presented. The algorithm makes use of high order interpolation for the function in space domain and with no approximation to the oscillatory kernel. This algorithm can achieve any large range of spectra with arbitrary frequency resolution without the restriction of the Nyquist sampling theorem. The accuracy of this algorithm is much better than traditional Discrete Fourier transform with comparable computation time in FFT; at the same time the number of sampling points required in the spatial domain can be greatly reduced. The computation cost of the proposed CFT algorithm is $O[(M+1)N\sum_{i=0}^{I-1}\log L_i]$. The algorithm is useful in computational electromagnetics and other areas where spectral methods are required.

ACKNOWLEDGMENT

CHZ, YS, and LJL are supported by the Natural Science Foundation of China (NSFC) under Grant 60901043.

APPENDIX A. PROOF OF LEMMA 1

Lemma 1: The finite Fourier transform of a monomial is

$$\int_{-1}^{1} t^m e^{-j2\pi ut}dt = e^w \sum_{s=0}^{m} \frac{(-1)^{m-s}m!}{(m-s)!}\frac{1}{w^{s+1}} - e^{-w}\sum_{s=0}^{m}\frac{m!}{(m-s)!}\frac{1}{w^{s+1}} \tag{A1}$$

where m is a non-negative integer.

Proof: Principle of Mathematical Induction is adopted here.

When $m = 0$, the left-hand side of (A1) can be rewritten into

$$\int_{-1}^{1} e^{-j2\pi ut} dt = \frac{e^{j2\pi ut}}{-j2\pi u}|_{t=-1}^{t=1} = \frac{e^{j2\pi u} - e^{-j2\pi u}}{j2\pi u} = \frac{e^{w} - e^{-w}}{w} \quad \text{(A2)}$$

and right hand of (A1) can be rewritten as

$$e^{w}\sum_{s=0}^{m}\frac{(-1)^{m-s}m!}{(m-s)!}\frac{1}{w^{s+1}} - e^{-w}\sum_{s=0}^{m}\frac{m!}{(m-s)!}\frac{1}{w^{s+1}}|_{m=0} = \frac{e^{w}-e^{-w}}{w} \quad \text{(A3)}$$

It is obvious that (A2) = (A3), so (A1) holds for $m = 0$.

Then we assume that for $m = S$, (A1) holds, or

$$\int_{-1}^{1} t^{S} e^{-j2\pi ut} dt = e^{w}\sum_{s=0}^{S}\frac{(-1)^{S-s}S!}{(S-s)!}\frac{1}{w^{s+1}} - e^{-w}\sum_{s=0}^{S}\frac{S!}{(S-s)!}\frac{1}{w^{s+1}} \quad \text{(A4)}$$

When $m = S + 1$, according to Newton Leibniz formula the left-hand side of (A1) is

$$\int_{-1}^{1} t^{S+1} e^{-j2\pi ut} dt = -\frac{t^{S+1}e^{-wt}}{w}|_{t=-1}^{t=1} + \frac{S+1}{w}\int_{-1}^{1} t^{S} e^{-wt} dt.$$

Substituting (A4) into the above equation, we obtain

$$\int_{-1}^{1} t^{S+1} e^{-j2\pi ut} dt = \frac{(-1)^{S+1}e^{w}}{w} - \frac{e^{-w}}{w}$$
$$+ e^{w}\sum_{s=1}^{S+1}\frac{(-1)^{S+1-s}(S+1-s)!}{(S+1-s)!}\frac{1}{w^{s+1}} - e^{-w}\sum_{s=1}^{S+1}\frac{(S+1)!}{((S+1)-s)!}\frac{1}{w^{s+1}}.$$

It is obvious that $\frac{(-1)^{S+1}e^{w}}{w} = \frac{(-1)^{S+1-0}(S+1)!}{(S+1-0)!}\frac{1}{w^{0+1}}$, $\frac{e^{-w}}{w} = \frac{(S+1)!}{(S+1-0)!}\frac{1}{w^{0+1}}$. Hence, (A1) holds when $m = S + 1$. So (A1) holds for all non-negative integer m.

APPENDIX B. ALGORITHM FOR COMPUTING $D_M^{(K)}$

For $M + 1$ different points $\{t_k\}_{k=1}^{M+1}$, $\{D_m^{(k)}\}_{m=0,k=1}^{M,M+1}$ are defined as $L_k(t) = \prod_{i=1,\ i\neq k}^{M+1}\frac{t-t_i}{t_k-t_i} = \sum_{m=0}^{M} D_m^{(k)} t^m$. To compute $D_m^{(k)}$, we define $l_0(t) = \prod_{i=1}^{M+1}(t-t_i) = \sum_{m=0}^{M+1} E_m t^m$, $l_k(t) = \prod_{i=1,\ i\neq k}^{M+1}(t-t_i) = \sum_{m=0}^{M} d_m t^m$. Hence,

$$l_k(t) = \frac{l_0(t)}{t-t_k} \quad \text{(B1)}$$

Computing cost for E_m is $O(M^2)$ [22]. According to (B1),

$$\begin{cases} d_M^{(k)} = E_{(M+1)} \\ d_m^{(k)} = E_{(m+1)} + d_{m+1}^{(k)} t_k, \ m = M-1, M-2, \ldots, 0 \end{cases} \tag{B2}$$

It requires M^2+M real multiplications to compute (B2). Then $l_k(t_k) = \prod_{i=1,\ i\neq k}^{M+1} (t-t_i) = \sum_{m=0}^{M} d_m t_k^m$ can be computed by the Horner scheme [21] with M real multiplications. It can be seen that $D_m^{(k)} = \frac{d_m^{(k)}}{l_k(t_k)}$. So $\{D_m^{(k)}\}_{m=0,k=1}^{M,M+1}$ can be computed with the cost of $O(M^2)$.

REFERENCES

1. Liu, Y. H., Z. P. Nie, and Q. H. Liu, "DIFFT: A fast and accurate algorithm for Fourier transform integrals of discontinuous functions," *IEEE Microwave and Wireless Components Letters*, Vol. 18, No. 2, 716–718, 2008.
2. Fan, Z., R. S. Chen, H. Chen, and D. Z. Ding, "Weak form nonuniform fast Fourier transform method for solving volume integral equations," *Progress In Electromagnetics Research*, Vol. 89, 275–289, 2009.
3. Semnani, A. and M. Kamyab, "Truncated cosine Fourier series expansion method for solving 2-D inverse scattering problems," *Progress In Electromagnetics Research*, Vol. 81, 73–97, 2008.
4. Huang, Y., Y. Liu, Q. H. Liu, and J. Zhang, "Improved 3-D GPR detection by NUFFT combined with MPD method," *Progress In Electromagnetics Research*, Vol. 103, 185–199, 2010.
5. Yang, S., Y. Chen, and Z. P. Nie, "Simulation of time modulated linear antenna arrays using the FDTD method," *Progress In Electromagnetics Research*, Vol. 98, 175–190, 2009.
6. Najjar-Khatirkolaei, B. N. and A. R. Sebak, "Slot antenna on a conducting elliptic cylinder coated by nonconfocal chiral media," *Progress In Electromagnetics Research*, Vol. 93, 125–143, 2009.
7. Liu, Y., Z. Liang, and Z. Yang, "Computation of electromagnetic dosimetry for human body using parallel FDTD algorithm combined with interpolation technique," *Progress In Electromagnetics Research*, Vol. 82, 95–107, 2008.
8. Swillam, M. A., M. H. Bakr, and X. Li, "Full wave sensitivity analysis of guided wave structures using FDTD," *Journal of Electromagnetic Waves and Applications*, Vol. 22, No. 16, 2135–2145, 2008.

9. Lei, J. Z., C. H. Liang, W. Ding, and Y. Zhang, "EMC analysis of antennas mounted on electrically large platforms with parallel FDTD method," *Progress In Electromagnetics Research*, Vol. 84, 205–220, 2008.
10. Froeyen, M. and L. Hellemans, "Improved algorithm for the discrete Fourier transform," *Review of Scientific Instruments*, Vol. 56, 2325, 1985.
11. Beaudoin, N. and S. S. Beauchemin, "A new numerical Fourier transform in d-dimensions," *IEEE Transactions on Signal Processing,* Vol. 51, No. 5, 1422–1430, 2003.
12. Sundararajan, D., *The Discrete Fourier Transform: Theory, Algorithms and Applications*, World Scientific Pub. Co. Inc., 2001.
13. Rabiner, L. R., R. W. Schafer, and C. M. Rader, "The chirp z-transform algorithm and its application," *IEEE Trans. Audio Electroacoust*, Vol. 17, 86–92, 1969.
14. Simonen, P. and H. Olkkonen, "Fast method for computing the Fourier integral transform via Simpson's numerical integration," *Journal of Biomedical Engineering*, Vol. 7, No. 4, 337–340, 1985.
15. Zeng, P., "High-accuracy formula for discrete calculation of fourier transforms," *Applied Mathematics and Computation*, Vol. 106, Nos. 2–3, 117–140, 1999.
16. Morelli, E. A., "High accuracy evaluation of the finite Fourier transform using sampled data," *NASA TM*, Vol. 110340, 1997.
17. Fan, G.-X. and Q. H. Liu, "Fast Fourier transform for discontinuous functions," *IEEE Transactions on Antennas and Propagation*, Vol. 52, No. 2, 461–465, 2004.
18. Liu, Y. H., Q. H. Liu, and Z. P. Nie, "A new efficient FDTD time-to-frequency-domain conversion algorithm," *Progress In Electromagnetics Research*, Vol. 92, 33–46, 2009.
19. Higham, N. J., *Accuracy and Stability of Numerical Algorithms*, Society for Industrial Mathematics, 2002.
20. Sarkar, I. and A. T. Fam, "The interlaced chirp z transform," *Signal Processing*, Vol. 86, No. 9, 2221–2232, 2006.
21. Graillat, S., P. Langlois, and N. Louvet, "Compensated horner scheme," Research Report, Vol. 4, 2005.
22. El-Mikkawy, M. E. A., "Explicit inverse of a generalized Vandermonde matrix," *Applied Mathematics and Computation*, Vol. 146, Nos. 2–3, 643–651, 2003.